ELSEVIER

Journal of Materials Processing Technology 92–93 (1999) 162–168

Journal of Materials Processing Technology

www.elsevier.com/locate/jmatprotec

The influence of small additions of Ni, Ti and C on the oxidation behaviour of sputtered tungsten coatings

C. Louro, A. Cavaleiro*

Departamento de Engenharia Mecanica, ICEMS-Faculdade de Ciências e Tecnologia da Universidade de Coimbra, Pinhal de Marrocos, Polo II, 3030 Combra, Portugal

Abstract

The oxidation rate of sputtered tungsten-based coatings, oxidised in air at temperatures of 600°C–800°C can be influenced significantly by the addition of small amounts of nickel, titanium and carbon. The presence of carbon does not change the type of oxide phases formed during the oxidation of sputtered W coatings: there are two oxide layers, the inner being a compact sub-oxide of WO_x type and the outer being a typical porous WO_3 phases. The addition of Ni and Ti, however gives rise, in addition to WO_x and WO_3, of other type of oxides, such as $NiWO_4$ and TiO_2, respectively. The oxidation process is very complex, with different fluxes of species to be considered: the oxygen ion flux from the exterior to the interior, and Ni and Fe diffusing towards the exterior. At the annealing temperature of 800°C, in the cases of W–C–Ni films, a $FeWO_4$ layer is detected beneath the mixed oxide. The greatest oxidation resistance is obtained for W–C–Ti, followed by W–C–Ni and finally W–C.

Keywords: Oxidation; Sputtering; Coatings; Tungsten

1. Introduction

The oxidation resistance of a material depends on the formation of a solid protective metal oxide film, which acts as a diffusion barrier and limits the rate of oxidation. The addition of different chemical elements to a material can improve the characteristics of the protective layer. Previous studies have shown that the addition of Ti and Ni have preponderant roles in the modification of the oxidation behaviour of sputtered coatings of W and W–N, either by forming the $NiWO_4$ spinel-type phase with much lower diffusion coefficients for oxygen ions, or by forming fine precipitates of titanium oxide, making the inward oxygen ion diffusion through the grain boundaries of the tungsten oxide layer difficult.

These films were developed to be used as hard coatings in mechanical applications in which high temperatures can occur. Despite the excellent mechanical properties of the coatings, their behaviour in service was not as good as expected. It was thought that the main cause of failure was the degradation of the coating by the high temperature oxidation process. Thus, detailed study of the oxidation behaviour of these coatings and the influence of these elements is fundamental.

This research work is a continuation of previous studies in order to try to understand the role of small additions of metallic elements Ti and Ni to sputtered W coatings with the simultaneous presence of carbon.

2. Experimental details

2.1. Deposition technique

The films were deposited by d.c. reactive magnetron sputtering with a specific target power density of 10 W cm^{-2} and a negative substrate bias of 70 V. Targets were W, W–10%Ti and W–10%Ni (mass fractions). The CH_4/Ar ratio of partial pressures was 1/5 and 1/3 for W–C–M (M = Ni, Ti) and W–C films, respectively. The substrates (5 mm × 5 mm × 1 mm) were of steel, and were polished down to a diamond paste of 1 μm. To completely coat the entire surface, the substrates were glued with precision in one of their lateral faces. Owing to the rotational movement of the substrate holder, all of the faces were coated uniformly. Before deposition, the sputtering chamber was evacuated by a turbomolecular pump down to a final pres-

*Corresponding author. Tel.: +351-39-790745; fax: +351-39-790701
E-mail address: albano.cavaleiro@mail.dem.uc.pt (A. Cavaleiro)

0924-0136/99/$ – see front matter
PII: S0924-0136(99)00222-8

sure of 10^{-4} Pa. The substrate surfaces were then ion cleaned by an ion gun. The cleaning procedure included an initial electron heating to temperatures close to 450°C and afterwards Ar^+ bombardment for 8 min (ion gun settings at 20 A, 40 V; substrates at −120 V). The deposition time was selected such as to obtain a final thickness of approximately 4 μm.

2.2. Characterisation techniques

Thermogravimetric tests were carried out on a Polymer Science Thermobalance of high resolution (0.1 μg). The oxidation temperature ranged from 600°C to 800°C, with a constant isothermal time of 30 min. The heating rate was selected as 30°C min^{-1}. Industrial air of 99.995% purity with a flow rate of 55 ml min^{-1} was introduced to the furnace during the oxidation tests.

A Cameca SX-50 electron probe microanalysis (EPMA) apparatus was used to determine the chemical composition of the coatings. The structure of the films was analysed by X-ray diffraction using a Siemens diffractomer with CuK_α radiation. The cross-section of the films obtained by fracturing the coated samples, the surface topology and morphological details were examined under a Jeol T330 scanning electron microscope (SEM) operated at 20 kV and at 0–15° view.

3. Results and discussion

3.1. Characterisation of the as-deposited films

Table 1 presents the results concerning the chemical composition, structure and morphology of the as-deposited W–C–M (M = Ni, Ti) films. Despite the same CH_4/Ar partial pressure ratio used in the deposition and the same content of Ni and Ti in the target, the carbon contents in the W–C–Ti films are greater than those in the W–C–Ni films. This is due to the higher affinity of Ti for carbon than Ni, as is explained as follows. Since the coatings are obtained with a negative substrate bias, during the deposition the lighter elements (C, Ti, Ni) are re-sputtered preferentially in comparison to W. Thus, lower contents of these elements should be expected in the films. This re-sputtering effect can be smoothed if the lighter elements are bonded to each other, making their sputtering during their stage as ''adatoms'' on the surface of the growing film more difficult. As the affinity of Ni for C is almost nil, there is no strong bonding formation between Ni and C allowing an easy preferential sputtering of both elements in relation to W. As a consequence, on the one hand, a lower Ni content in the film is measured in comparison to that of the target, and on the other hand W–C–Ni films present lower contents of Ni and C in relation to Ti and C of W–C–Ti films.

W–C–Ti coatings present more compact morphologies (they are featureless) according to Thornton's classification [1] than W–C or W–C–Ni, which have morphologies of type 1. All of the films revealed the presence of a unique phase, the b.c.c. α-W [2] with a strong (1 1 0) orientation, although the equilibrium diagram indicates very low solubility of carbon in tungsten. Thus, the C should be in a metastable position in the b.c.c. tungsten matrix, which explains the shift observed in the X-ray diffraction peaks relative to the equilibrium structures.

3.2. Oxidation and weight gain measurements

The isothermal mass change data for the coated samples are presented in Fig. 1. For 600°C oxidation temperature, all of the coatings present incipient oxidation with weight gains of less than 0.25 mg cm^{-2}. As expected, with temperature increase, greater oxidation rates were observed. Some remarks emerge from the observation of these curves, as follows:

1. The behaviour of W–C and W–C–Ni coatings is very similar at 600°C and for the first step at 700°C only after some annealing time at 700°C, is a sudden improvement in the oxidation behaviour of W–C–Ni observed. Such behaviour means that another oxidation mechanism, different from that observed for W–C films, should take place at 700°C.
2. W–C–Ti films presents the best oxidation resistance of all of the coatings studied.
3. W–C films show a sudden decrease of the weight gain for the 800°C oxidation temperature, As will be explained later, this is due to the mechanical instability of the oxide layers and to their flaking from off the coated sample as well as their loss from the sample holder.

The oxidation behaviour for W–C and W–C–Ti appears to be well described, at least in the initial stages

Table 1
Chemical composition, structure and morphology results of as-deposited sputtered W–C–M (M = Ni, Ti) films

W–C–M film	Chemical composition by EPMA (at %)			Structure (X-ray diffraction)	Morphology (cross-section)
	W	Ti or Ni	C		
W–C	93.5 ± 0.3	–	6.5 ± 0.3	α-W	1
W–C–Ni	87.9 ± 0.1	4.7 ± 0.1	7.4 ± 0.1	α-W	1
W–C–Ti	81.0 ± 0.3	10.8 ± 0.2	8.2 ± 0.2	α-W	Featureless

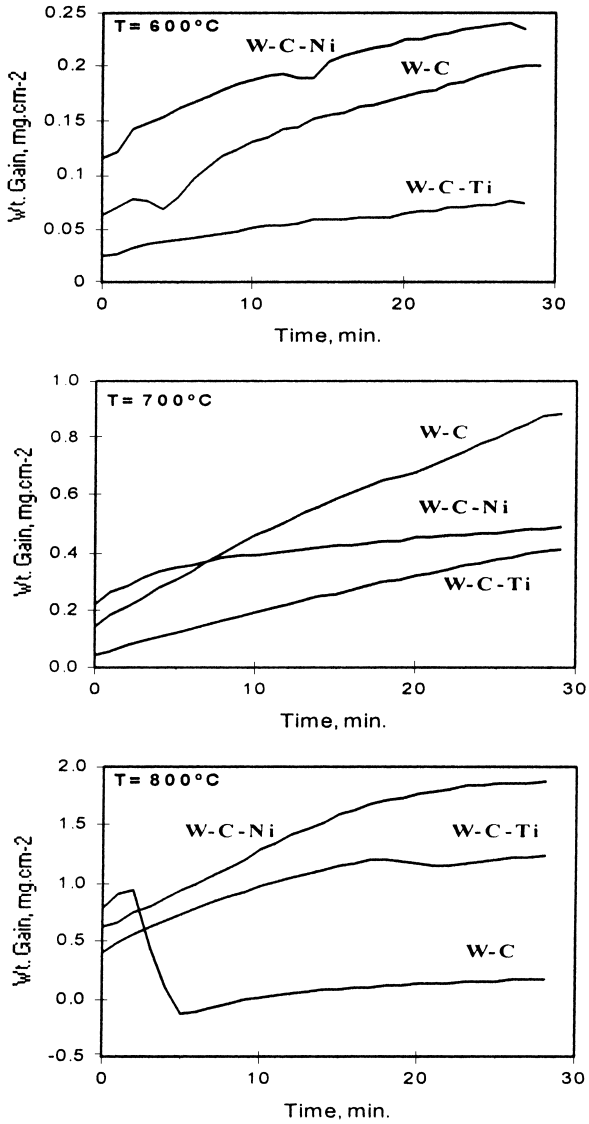

Fig. 1. Isothermal oxidation of W–C–M (M = Ni, Ti) films in air.

of oxidation, by a parabolic growth law that can be expressed as [3,4]

$$\left(\frac{\Delta m}{A}\right)^2 = k_p \times t, \tag{1}$$

where Δm is the weight gain, A the reactive area, K_p the parabolic rate constant and t is the oxidation time. The values of the parabolic oxidation constant obtained are listed in Table 2.

In the case of W–C–Ni (see Table 3), two parabolic oxidation behaviours can be distinguished: one considering the entire annealing at 600°C and the beginning of the entire annealing at 700°C; the other considering the last steps at this temperature and the beginning at 800°C annealing temperature.

The temperature dependence on the oxidation reaction can be represented by the Arrhenius-type equation [3,4]

Table 2
Values of the parabolic oxidation constant, K_p[a]

$K_p \times 10^{-2}$ mg^2 cm^{-4} min^{-1} (time/min)		
T (°C)	W–C	W–C–Ti
600	0.14 (30)	0.02 (30)
700	2.69 (30)	0.73 (30)
800	21.94 (2)	7.93 (2)

[a] Parabolic times shown in parentheses.

$$k_p = A \exp\left(-\frac{E_a}{RT}\right), \tag{2}$$

where A is a constant, T the isothermal oxidation temperature and E_a is the apparent activation energy. The values of the apparent activation energy obtained are listed in Table 4.

For W–C–Ni films two apparent activation energy values are presented corresponding to the above-mentioned oxidation regimes. The analysis of E_a values allows the confirmation of the similarity between the behaviour of W–C and W–C–Ni for low oxidation temperatures. Moreover, it is possible to conclude that both W–C–Ni (higher temperature) and W–C–Ti films have different limiting oxidation mechanisms from those of the other cases.

3.3. Structural analysis

The structural analysis of the reaction products resulting from the coating oxidation is shown in Fig. 2, which presents the XRD spectra at increasing oxidation temperatures. The oxidation of W–C films, concerning the type of oxides formed, is similar to that observed for single tungsten coating [5], i.e., it is possible to distinguish: (i) a compact internal layer which is indexed as WO_x [6], as has been explained before [7]; an external layer resulting from the

Table 3
Values of the parabolic oxidation constant, K_p[a]

$K_p \times 10^{-2}$ mg^2 cm^{-4} min^{-1} (time/min)	
T (°C)	W–C–Ni
600	0.16 (30)
700	1.57 (4)
700	0.46 (20)
800	8.77 (2)

[a] Parabolic times shown in parentheses.

Table 4
Values of apparent activation energy, E_a

Film	E_a (kJ mol^{-1})
W–C	197
W–C–Ni (low temperature)	161
W–C–Ni (higher temperature)	256
W–C–Ti	234

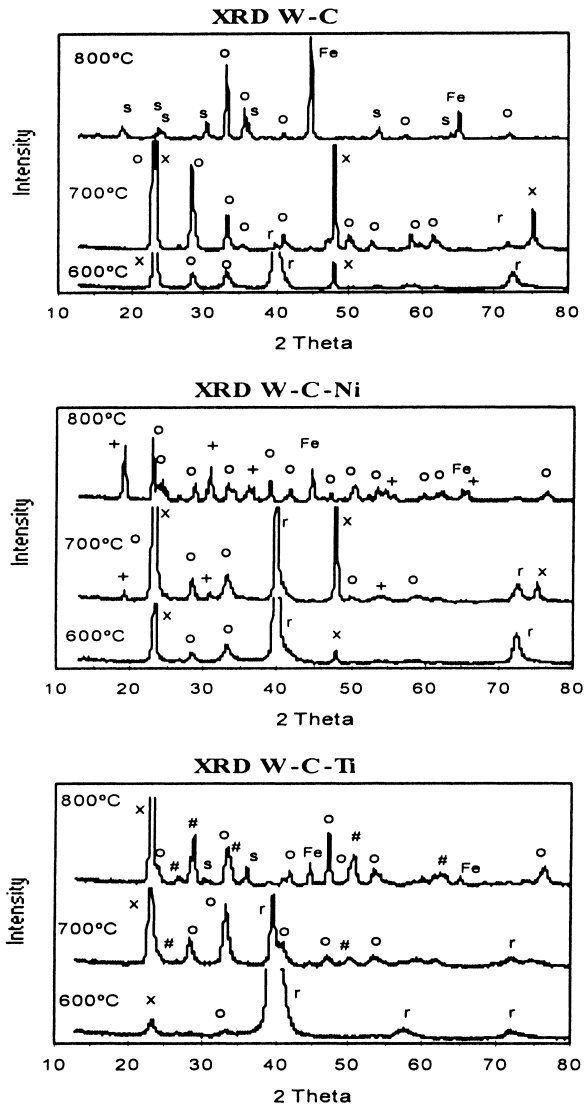

Fig. 2. Structural evolution of W–C–M (M = Ni, Ti) films with oxidation temperature; (o) WO_3; (x) WO_x; (+) $NiWO_4$; (#) TiO_2/Ti_3O_5; (s) $FeWO_4/Fe_2O_3/Fe_3O_4$; (r) unoxidised coating.

transformation of WO_x to WO_3 (which is yellow and porous) [6].

For 800°C, in agreement with the observations presented above, the oxidised samples reveal a great amount of oxides related to the substrate (α-Fe, Fe_2O_3, $FeWO_4$ and eventually Fe_3O_4 [8]). This is due to the flaking off of the oxidised coatings, as was demonstrated by the sudden decrease observed in the weight gain curve (see Fig. 1).

In the case of W–C–Ni, the greater oxidation resistance when compared to W–C can be explained by the formation of the mixed oxide $NiWO_4$ [9]. This phase is detected for temperatures greater than 700°C. Only for these temperatures do the W–C–Ni coatings shows a better oxidation behaviour than that of W–C films. As was suggested in a previous paper [7], the efficiency of this layer is only valid if its thickness in relation to the WO_x oxide reaches a threshold value. It seems that this happens only after a particular time at 700°C. In fact, at the beginning of the isothermal annealing, the upwards diffusion of Ni is not enough to form a thick $NiWO_4$ layer. When this behaviour is compared with that presented in a previous work for W–Ni and W–N–Ni coatings [7], it is possible to conclude that the carbon should have a preponderant role in perturbing the diffusion of Ni in the W matrix. Effectively, in the study for those coatings containing Ni, it was possible to detect immediately the formation of $NiWO_4$ at 600°C, although in the case of W–Ni, the nickel content was lower than that evaluated for W–C–Ni films. In the same study only one E_a value was found, taking into consideration all the annealing temperatures. This result ($E_a = 180\ kJ\ mol^{-1}$) was close to that determined for W–C–Ni at lower temperatures, confirming that effectively after some time at 700°C the spinel-type $NiWO_4$ formation should take place at a sufficiently higher rate to be predominant in relation to the WO_x formation. Moreover, it is also important to remark that for 800°C, annealing diffusion of iron upwards should take place, because by EDXS it was possible to find a concentration of this element in the inner part of the $NiWO_4$ layer, suggesting the formation of the $FeWO_4$ oxide. This behaviour was not observed for W–Ni and W–N–Ni coatings.

As indicated by thermogravimetric analysis, W–C–Ti films present the best oxidation behaviour. Moreover, the apparent activation energy value that is determined is equal to that found in a previous study for W–Ti single films [7]. This suggests a similar oxidation behaviour for these coatings, which substantiates the authors previous explanation when comparing the W–N–Ti and W–Ti films. In that research work the higher oxidation resistance of W–Ti films is attributed to the fine precipitation of Ti oxides on the intergranular boundaries of the oxide layer. The titanium oxide precipitation would only be possible if this element were oxidised preferentially and this would only be thermodynamically favourable if the Ti were in solid solution in the W matrix. This was not observed for W–N–Ti coatings, for which the formation of mixed nitrides of W and Ti were formed in the as-deposited films. As the structure of W–C–Ti is also b.c.c. α-W phase, the preferential oxidation of Ti and an oxidation behaviour similar to W–Ti coatings should be expected. The analysis of Fig. 2 confirms this. Indeed, the structural evolution of the oxides is similar to that formed for W–Ti, either for the TiO_2/Ti_3O_5 [10] detection or for the tungsten oxides.

3.4. Morphological characterisation

The morphological observation of the oxide layers allows the confirmation of some of the comments referred to above. Thus, Fig. 3 shows that W–C films oxidise by layers, the inner layers being more compact than the outer layers.

At 800°C, extensive spalling of the oxide layer is observed. Some signs of oxide layer degradation in the form of small eruptions are already observed at 700°C (Fig. 4). This behaviour can be explained by considering

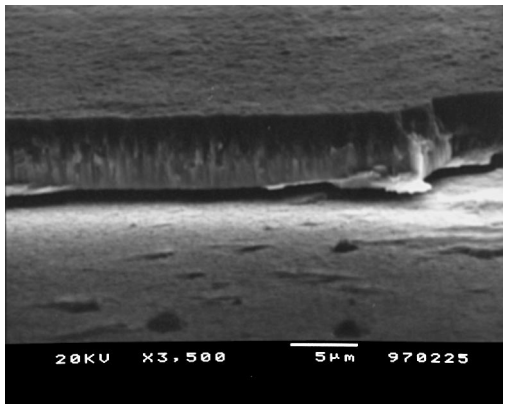

Fig. 3. SEM micrograph of cross-section W–C films oxidised at 700°C for 30 min.

on the one hand the formation of CO or CO_2 at the interface of oxide metal, and on the other hand the very high Pilling–Bedworth relationship, which expresses the difference on the molar volume between WO_3 and W–C, that leads to crack propagation and spalling when the oxide layer thickness exceeds a threshold value. The association of these two factors leads to the strong flaking of the oxide.

This phenomenon was observed a long time ago, during the oxidation of W–C alloys [11]. The oxidation of W–C–Ni by layers is demonstrated by the SEM micrograph of cross-sections shown in Fig. 5. Analysis by EDXS (Fig. 5(b)) on the top layer shows a high Ni content, confirming that nickel rapidly enriched the surface, forming a two-phase structure: a thin external layer of $NiWO_4$, followed by three internal layers, one of tungsten–iron oxide followed by two of tungsten phases. The phenomenon of the local oxide layer degradation is also observed for W–C–M (M = Ni, Ti) coatings (see Figs. 6 and 7) where numerous ''cauliflower's'' features are shown.

The EDXS analysis of the centre of the zones in Fig. 6 shows that the Ni content is much higher than that in other zones, which means that the oxidation stage is well advanced. This type of punctual oxidation seems different from that observed for W–N–Ni coatings [12]. Indeed, in

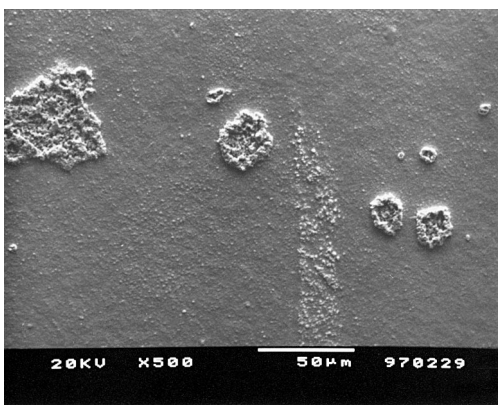

Fig. 4. SEM micrograph of W–C films oxidised in air at 700°C for 30 min.

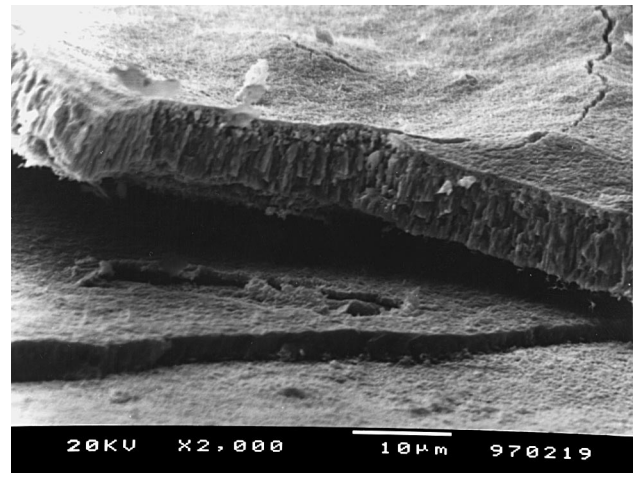

Fig. 5. Presenting: (a) an SEM micrograph of the cross-section of W–C–Ni films oxidised at 800°C for 30 min; (b) an EDXS analysis (at %).

this latter case, the preferential oxidation occurred in the places where the structural transformation amorphous → crystalline began to take place. The volume variation during this transformation gave rise to the degradation of the oxide layer in that zone and consequently to a higher oxidation rate. As has been referred to above, the W–C–Ni films that have been analysed in this work, have a crystalline structure. Thus the oxide degradation should not be attributed to any structural transformation but, similar to what was described above for W–C coatings, to a mechanical instability of the oxide layer due to CO/CO_2 liberation and/or the high Pilling–Bedworth ratio of this system.

Similarly, as for W–Ti films [5], in W–C–Ti samples it was not possible to detect, by EDXS, titanium agglomerations corresponding to the Ti–O particles. The cross-sectional analysis showed only a main oxide layer, much more compact than those observed for W–C films. An interesting feature showing that the upwards diffusion of the iron from the substrate is enhanced by EDXS analysis is represented schematically in Fig. 8(b). It is possible to conclude that there are zones in the oxide layer that are richer in Fe than the layer closest to the substrate.

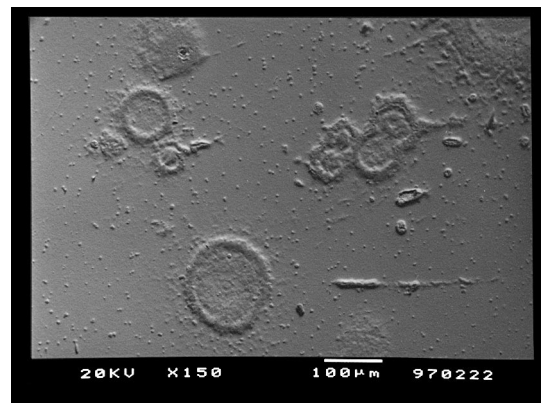

Fig. 6. SEM micrograph of the surface morphology of W–C–Ni films at 700°C oxidation temperature.

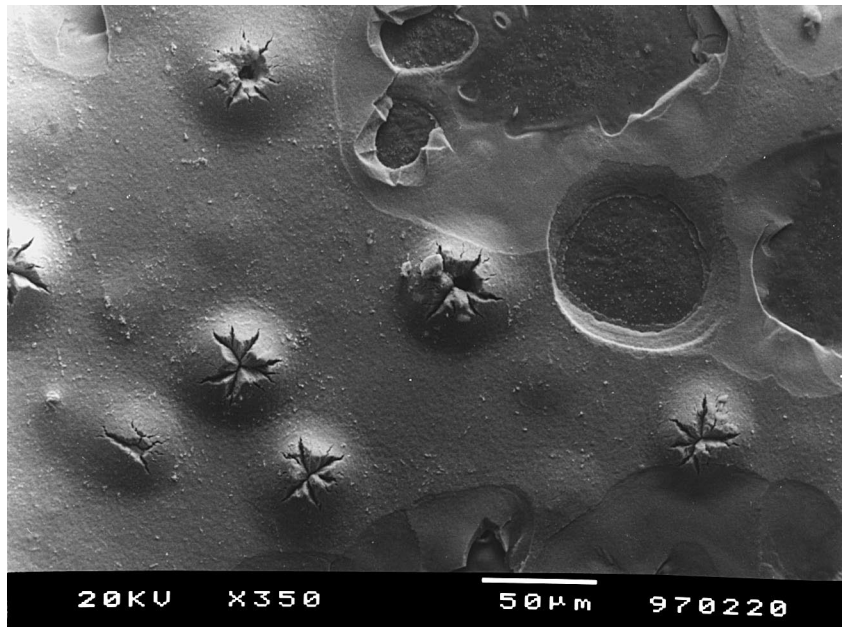

Fig. 7. SEM micrograph of the surface morphology of W–C–Ti films oxidised at 800°C for 30 min.

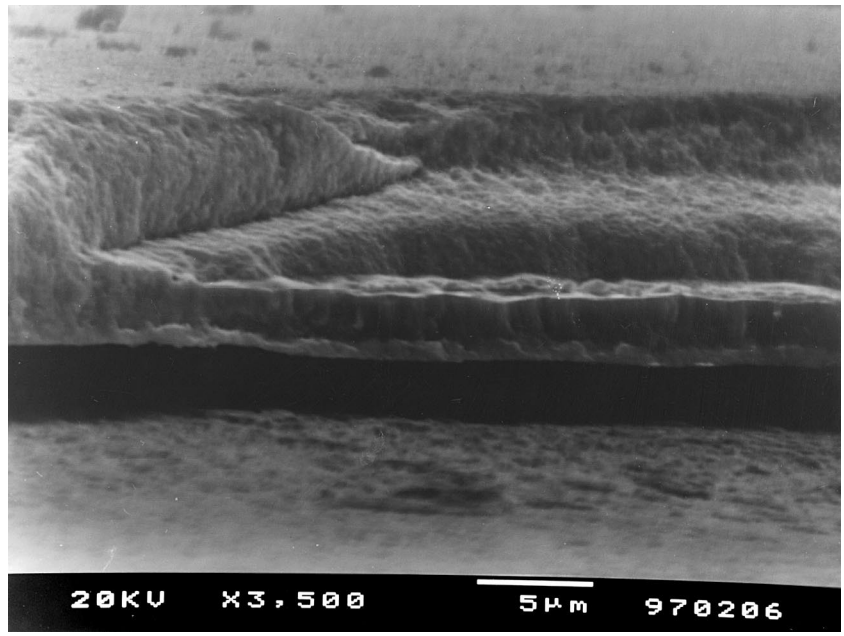

Fig. 8. Presenting: (a) an SEM micrograph of the cross-section of W–C–Ti films at 800°C oxidation temperature; (b) an EDXS analysis (at %).

4. Conclusions

Detailed characterisation of the oxidation behaviour of sputtered W–C–M (M = Ni and Ti) coatings has led to the following conclusions:

1. The incorporation of carbon during the sputtering process increases the oxidation resistance when compared with films without the addition of this element.
2. In the range of temperature studied, all of the coatings show a parabolic oxidation behaviour, which suggests a process controlled by ion diffusion through the oxide layer.
3. Small additions of Ni and Ti to sputtered W–C coatings can significantly improve the oxidation resistance.
4. All of the films studied oxidise by layers, forming oxides with different structures and chemical compositions. The good oxidation resistance of W–C–Ti films is attributed to the formation of titanium oxides, which obstruct the inwards diffusion of oxygen ions. For nickel-containing films, which present two distinct oxidation mechanisms, the formation of an external layer of a mixed oxide

($NiWO_4$) also gives rise to an excellent oxidation behaviour, since this spinel acts as a barrier to the diffusion of oxygen ions.

References

[1] J.A. Thornton, Annu. Rev. Mater. Sci. 7 (1977) 239.
[2] Joint Committee on Power Diffraction Standards, Power Diffraction File, International Centre for Diffraction Data, Swarthmore, PA, Cards 4-0806.
[3] M.G. Fontana, N.D. Greene, Corrosion Engineering, McGraw-Hill, chapter 11, New York, 1978.
[4] J.P. Chilton, Principles of Metallic Corrosion, 2nd ed., chapter 9, The Chemical Society, London, 1973.
[5] C. Louro, M.Sc., Thesis, Coimbra University, 1995.
[6] Joint Committee on Power Diffraction Standards, Power Diffraction File, International Centre for Diffraction Data, Swarthmore, PA, Cards 5-0392, 36-0101, 5-0058, 5-0386, 36-0103, 20-1323, 20-1324, 24-074, 32-1394, 32-1395, 33-1387, 41-0369.
[7] C. Louro, A. Cavaleiro, J. Electrochem. Soc. 144 (1997) 259.
[8] Joint Committee on Power Diffraction Standards, Power Diffraction File, International Centre for Diffraction Data, Swarthmore, PA, Cards 6-0696, 15-0615, 27-0256, 19-0629.
[9] Joint Committee on Power Diffraction Standards, Power Diffraction File, International Centre for Diffraction Data, Swarthmore, PA, Cards 15-0755.
[10] Joint Committee on Power Diffraction Standards, Power Diffraction File, International Centre for Diffraction Data, Swarthmore, PA, Cards 21-1276, 31-0180, 40-0806.
[11] W.W. Webb, J.T. Norton, C. Wagner, J. Electrochem. Soc. 103 (1956) 112.
[12] C. Louro, A. Cavaleiro, Surface, Coatings Technol. 74–75 (1995) 998.